Graphical abstract

Gold nanoparticles in different sizes are deposited into wire arrays through discontinuous Vertical Evaporation-driven Colloidal Deposition (dVECD) for electronic sensing of biological molecules. Because of the high surface-to-volume ratio, gold nanoparticle wires are able to achieve a sensitive label-free detection of DNA molecules as well as their interactions with proteins.
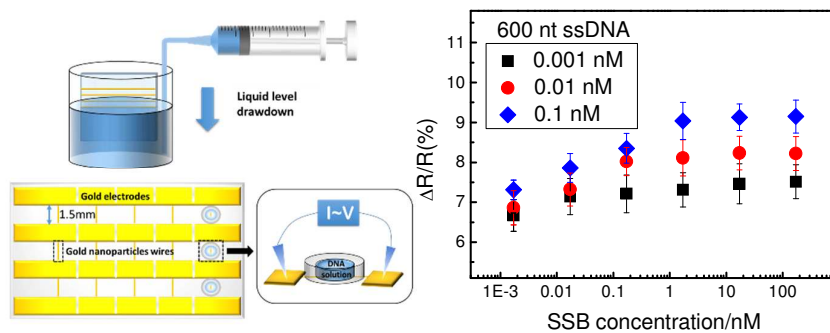
Gold nanoparticle wires for sensing DNAs and DNA/protein interaction

Liqin Shao,[a] J. J. Diao,*[c] Zhipeng Tang,[a] Song Liu,[a] Sophie C. Shen,[d] Jiankang Liu,[c] Xianfeng Rui,[e] Dapeng Yu[ab] and Qing Zhao*[ab]

The discontinuous Vertical Evaporation-driven Colloidal Deposition (dVECD) has been used as a green technique for formatting nanoparticle wires by the direct deposition of nanoparticles from colloid suspensions onto hydrophilic substrates, without any lithographic procedures. Gold nanoparticles in different sizes are deposited into wire arrays for electronic detections of biological molecules. A sensitive detection of DNA molecules as low as ~ 1 pM is achieved due to high surface to volume ratio of the porous structures. The effects of gold nanoparticle size, DNA concentration, and DNA length on detection sensitivity of these gold nanoparticle wire sensors are discussed. Moreover, we can also detect the interaction between DNAs and proteins. Gold nanoparticle wires prepared by the nontoxic and simple dVECD are promising for detecting virus involved in diseases.

Nanoscale Accepted Manuscript

Introduction

Scientists have put tremendous efforts into nanoparticle research for many unique properties of nanoparticles,[1,2] which could be assembled into various bulk structures for real applications.[3,4] Technical developments for the precise assembly of nanoparticles into functional structures have become an exciting research area for potential nanotechnology applications.[5] Existing methods based on lithography can either directly put nanoparticles in the array shape or provide a platform for nanoparticle assembly.[6-11] Meanwhile, single-step assembly methods, such as dielectrophoresis, are also attractive, despite the limited control of their resulting structures.[12] Approaches for nanoparticle assembly foresee the new advanced materials and have attracted tremendous attention for applications such as electronic biomolecule sensors.[13-16] Compared to complicated biomolecule sequence detection, such electronic measurement can be a much easier testing method. Thus, in recent years, large amounts of efforts on technical developments on simplicity, scale, resolution, and cost have been applied to producing 1-dimensional nanoparticle structures.[17-22]

Meanwhile, due to the environmental pressure, the demand of green manufacturing techniques to reduce or eliminate the use or generation of hazardous substances has been significantly increased.[23] With inspiration from natural de-wetting phenomena, such as coffee ring stains, by which colloidal particles in the solution move to the air-liquid-solid interface with a tendency, discontinuous Vertical Evaporation-driven Colloidal Deposition (dVECD) has been designed for the assembly of colloidal particles.[20] Despite hazardous materials involved in nanoparticle synthesis, this method itself has been regarded as a greener effort, which reduces or eliminates the use or generation of hazardous substances.[24] Furthermore, this method is versatile for depositing both metallic and nonmetallic nanoparticles, under different solvent and substrate conditions.

Because of the nice biocompatibility and a strong dependence of the electronic property on the capping molecules,[25, 26] gold nanoparticles have been chosen as ideal building blocks to

Nanoscale Accepted Manuscript

form nanoparticle wires for sensors. Due to the large surface area offered by porous nanoparticle structures, electronic detections of chemical molecules[27] and strain[28, 29] with a high sensitivity have been achieved.

In this paper, by using gold nanoparticle wires fabricated by discontinuous Vertical Evaporation-driven Colloidal Deposition, we demonstrate the application in the highly sensitive electronic detection of biological molecules, DNAs. Moreover, these porous nanoparticle wires are also able to sense the interaction between DNA and protein in a label-free manner.

Results and discussion

Discontinuous Vertical Evaporation-driven Colloidal Deposition (dVECD)

The dVECD creats a set of discrete wires parallel to the three-phase meniscus contact line. The width and height of the wires lie on the colloidal suspension temperature, and the deposition time, as discussed elsewhere.[30] Fig. 1a illustrates a schematic of the experimental setup. The deposition process of dVECD is operated at room temperature and atmospheric pressure. The deposition setup was fixed on a shock-absorbing platform. A hydrophilic quartz substrate was vertically immersed in the gold nanoparticle dispersion and kept stationary. With the solution level lowered, driven by the liquid-solid-gas interface force and the evaporation, the gold nanoparticles were accumulated at the solid-liquid-gas interface region to form a wire-like structure.[31] While uninterrupted evaporation brings a continuous nanoparticle thin film,[27, 32, 33] evaporation followed by a rapid decline of the liquid level leads to the formation of a nanoparticle wire (Fig. 1b). The repetition of this process causes formation of numerous parallel nanoparticle wires on the substrate. The interval distance between wires was controlled by withdrawing appropriate liquid from the suspension through the injection syringe. Here, withdrawing of 1 ml solution can result in a 1.5 mm interval distance. The width of the wire depends on the deposition time, which was optimized to 10 min for all gold nanoparticle wires (GNPWs) with width of 12 μm used in this paper.

Nanoscale Accepted Manuscript

Gold nanoparticle wire formation

Fig. 2a and 2b are optical microscope images of the deposited parallel-patterned gold nanoparticle wires, which is perpendicularly to the direction of the liquid descending level, i.e. parallel to the air-liquid-substrate three phase contact line. The width of the wire is ~12 μm and the height is ~60 nm according to atomic force microscope (AFM) measurements (Fig. 2c), with the interval distance between nearby wires of 1.5 mm. The results indicate that dVECD is an effective and flexible method to fabricate parallel nanoparticle wires separated by a tunable distance, which interestingly realize the coexistence between microscale periodicity and nanoscale ordering. Note the particle wire can be made very long, up to the width of the substrate used. And the wire is continuous with no cracks observed all cross its length and width. The AFM cross section image in Fig. 2c shows that the nanoparticles in wire are multilayered, with thickness increasing from one edge to the other. The wire starts to grow from its thin side, facing the dry region of the substrate, leading to the asymmetry shape of the image. Gold nanoparticle size can be precisely tuned via a method reported by Neus G. Bastus.[34] By changing nanoparticle size, various conducting wires can be made with different surface morphologies. Fig. 2d-f show typical transmission electron microscope (TEM) images of three different particle size of 14.01 ± 1.68 nm, 26.57 ± 2.69 nm and 36.64 ± 2.43 nm, respectively. The corresponding surface morphology of gold nanoparticle wires were illustrated by scanning electron microscopy (SEM) in Fig. 2g, 2h, and 2i, respectively. Gold nanoparticles are closely stacked with each other when forming into wire structure. Smaller nanoparticles form a better-packed structure with smaller sizes of gaps between nanoparticles (Fig. 2g, 2h, and 2i), which directly correlates to the performance of GNPWs. The gap between gold nanoparticles follows a near proportional relation to the size of nanoparticles (14 nm GNPWs: 0 ~ 10 nm, 27 nm GNPWs: 10 ~ 20 nm, 37 nm GNPWs: 20 ~ 30nm).

Following an annealing process for compacting nanoparticles (please see Fig. S1 in the ESI†), GNPWs were exposed to a 10 mM 1-dodecanethiol (DDT) in ethanol for 12 h, which

neutralizes the surface charge of gold nanoparticles.[35] The resistance of gold nanoaprticle wires increased after DDT treatment, in agreement with previous study after ODT treatment.[27] Moreover, this DDT treatment also increases the roughness of GNPWs (Fig. 3), which could further benefit the sensitivity.[27] After that, GNPWs were electrically connected to gold electrodes by the electron beam evaporation, and then the resistance was measured by a semiconductor parameter analyzer through a probe station system (Fig. 4a). The resistance of GNPWs (500 ~ 2000 Ω) was significantly larger than the contact resistance of gold electrodes, and hence our observations are mainly contributed from GNPWs. Small reservoirs made from polydimethylsiloxane (PDMS) were attached to GNPWs for containing liquid samples. Fig. 4b illustrates the detailed approaches for sensing chamber formation, electrode connection, small reservoir attachment, and electric sensing of biomolecules. First the substrate with prepared gold nanoparticle wires was supported by other three pieces of glasses ("carriage" in inset of Fig. 4b) to form a chamber to use the wires from both sides of the substrate (Fig. 4b①). Then several gold electrodes perpendicular to GNPWs were evaporated onto the substrate surface (Fig. 4b②). Then the gold electrodes were mechanically divided into electrode segments along the parallel direction with wires at places in between nearby gold nanoparticle wires (the cutting trace on gold electrodes was marked as silver sign in Fig. 4a) to form pattern of many independent devices with two gold electrodes and the wire connecting them, as indicated as a black square in Fig. 4a. Subsequently small reservoirs were attached to GNPWs between two adjacent electrodes for biomolecule solution loading (Fig. 4b③ and the zoom-in scheme of the black square in Fig. 4a). Tens of these small GNPW sensor devices can be easily fabricated on the substrate through the versatile design (six of them are shown in Fig. 4b③), which is beneficial for batch production. The electrical measurement was conducted before and after DNA injecting into reservoir through a probe station system (Fig. 4b④).

DNA sensing

The electronic properties of gold nanoparticles can be influenced significantly by surrounding environment, such as the surface capping agents.[36] Meanwhile, many reports have shown that large biological objects such as protein and virus can alter the electric behavior of nanowires.[37,38] With a high surface-to-volume ratio caused by the porosity (Fig. 2),[27,39] the conducting GNPWs appear promising in sensitive electronic detections for biological objects.

The performance of the fabricated GNPWs was evaluated by adding DNA molecules in different concentrations and sizes to a small reservoir attached to GNPWs and electrode (Fig. 4) for monitoring the variation of the electrical resistance of GNPWs. After adding the buffer (10 mM Tris, 50 mM NaCl, pH 8.0) as a background check with no resistance change, 0.001, 0.01, 0.1, 1, and 10 nM double-stranded DNAs (dsDNAs) were added sequentially. Resistance decrease was observed after sample addition. The relative resistance variation ($\Delta R/R$) as a function of DNA concentration with different DNA lengths (600, 1200, and 3200 base-pairs (bp)) was shown in Fig. 5. Each point in Fig. 5 was the values measured by 10 GNPWs in the same sensor with standard deviation. The detection limit is ~ 0.001 nM, which is an order of magnitude lower than the previous report.[40] As shown in Fig. 5, for different size of dsDNAs, a larger resistance change was caught for shorter DNAs. For example, the $\Delta R/R$ value reaches ~ 9 % for 10 nM 600 bp DNAs, while 4.3 % is caught for 10 nM 3.2 kbp DNAs (Fig. 5b). In addition to DNA concentration and length, we also tested the effect of gold nanoparticle size in detection sensitivity. As shown in Fig. S2 (supporting information), for different sizes of gold nanoparticles (14, 27, and 37 nm), GNPWs made of bigger gold nanoparticles gave a larger resistance change (for all three lengths under five measured concentrations). For example, we observed ~ 8% of the $\Delta R/R$ value for 37 nm GNPWs, and ~ 2 % for 14 nm GNPWs (Fig. S2b).

The above result demonstrates that DNA molecules bridge gaps of nanoparticles to change the resistance (Fig. 5d). The insertion of shorter DNAs into nanoparticle gaps gives a larger

Nanoscale Accepted Manuscript

resistance variation. For GNPWs made of larger nanoparticles, we also found more resistance changes. These results can be explained by the percolation theory.[41] Based on that theory, the electron transport in GNPWs is caused by single electron tunneling, which occurs across the gap distance between adjacent gold nanoparticles. After DDT neutralization, the gold nanoparticles led to reorganization and form small clusters. Therefore, the formation of large gap between the small clusters strengthens the gap separation disorder, which affects the conductivity of the GNPWs.[35] DNAs can be regarded as random immobile offset charges between gold nanoparticles resulting in local charge disorder.[41] The offset charge disorder plays an important role on the resistance of GNPWs by influencing the Coulomb blockade voltage, V_b.[42] Individual DNA molecule behaves a wide bandgap semiconductor property,[43] while an aligned anisotropic DNA films performs a linear conductor character.[44] When DNA molecules insert into gaps between gold nanoparticles, they disturb the offset charge. As the result of local charge disorder, the resistance of GNPWs varies upon DNA insertion. Moreover, the more DNAs get percolated in nanoparticle gaps, the higher degree of offset charge disorder could be achieved for giving a greater V_b value change.[42] As shown in Fig. 2g-i, larger nanoparticle size results in larger nanoparticle gap inside each wires, therefore, the larger nanoparticle gap would allow more DNAs to percolate in nanoparticle gaps, leading to larger resistance change (Fig. 5a-c). For shorter DNA length, there should be more DNAs percolate in nanoparticle gaps compared to longer ones, where large parts of them wander around the surface and cannot percolate into gaps (Fig. 5d). Therefore, shorter DNAs could cause a larger resistance change (Fig. S2).

Mathematically, according to the percolation theory, the resistance reduction ΔR of GNPWs is given by: $\Delta R = R - R' = R_0 e^{\xi_c}$, where R and R' are the resistance value before and after DNA testing; ξ_c is a value at the percolation threshold, which is related to the widths of separation gap distribution and Coulomb energy distribution; R_0 can be seen as constant.[41] Our results shown in Fig. 5 fit into the exponential rule at low concentrations, and get

saturated at a high concentration, which is due to the limited number and size of gaps between nanoparticles.

Detection of DNA/protein interaction

DNA-induced local charge disorder is also sensitive to local environmental changes around DNAs, such as protein binding. Single-stranded DNA binding (SSB) protein was used to demonstrate the capability of GNPWs in detecting biomolecular interactions, for instance, between DNA and protein. In the T50 buffer (10mM Tris-HCl, 50mM NaCl, pH 9), two of the SSB subunits bind to 35 nucleotides (nt) of single-stranded DNAs (ssDNAs).[45] As a control, we showed that the influence from SSB alone is negligible: the resistance change of GNPWs is insensitive to the concentration change of SSB (Fig. 6a). In our experiments, ssDNAs formed by unwinding dsDNA molecules at 90 ^{o}C followed by a rapid cooling to room temperature, were explored to SSB molecules for complex formation (Fig. 6b). Note that detection only ssDNA with GNPWs is not easily achieved under the same condition as SSB since ssDNAs are unstable at pH 9 under room temperature. In the presence of ssDNA, we can see the $\Delta R/R$ value starts to change upon adding of SSB, in a dose-dependent manner (Fig. 6c, 6d, and 6e). Each point in Fig. 6 was the values measured by 10 GNPWs in the same sensor with standard deviation. For example, the $\Delta R/R$ value reaches 6.6 % for 600 nt ssDNAs (0.001 nM) binding SSB (0.001 nM) and gets saturated when SSB concentration increases to 0.01 nM with the value of 7.1 %. While the $\Delta R/R$ value reaches saturation at 1 nM SSB when 0.1 nM 600 nt ssDNAs was used (Fig. 6c). The saturation phenomenon is due to that a certain concentration and length of ssDNA can only bind the explicit amount of SSB. With higher concentration or longer ssDNAs lead to the greater saturation SSB concentration value as we can see in Fig. 6d and Fig. 6e. In the same way, more significant change was observed for smaller ssDNA molecules, which agrees with the percolation theory discussed above. Note that a very low concentration of both ssDNA and SSB (< 1 pM) can be detected with observable $\Delta R/R$ value in our gold nanoparticle wire sensor. Our GNPWs-based sensors

for the interaction between DNA and protein demonstrate a higher sensitivity over the thin nanoparticle film with huge gaps.[46]

Conclusions

In conclusion, gold nanoparticle wires have been successfully prepared by discontinuous VECD technique, a simple, green, and versatile method without any lithographic process for wide uses. Those conducting GNPWs made of different size of nanoparticles are used for the label-free electronic detection of biomolecules. The GNPW-based biosensors can not only detect various concentrations of DNAs, but also sense the interaction between DNA and protein. A strong dependence of DNA length and nanoparticle size in detection sensitivity was found: shorter DNA length and larger nanoparticle size give better detection sensitivity. A low concentration of biomolecules (~1 pM) can be detected with a large resistance change comparable to previous report,[47] without involving lithography process. Because of the high surface-to-volume ratio, these porous nanostructures foresee a potential for sensitive electronic detections of molecules involved in diseases. Moreover, since the gaps between nanoparticles are important for electronic sensing, one would expect a better sensitivity for nanoparticle wires by using nanoparticles with irregular shape, such as nanostars.

Experimental

Materials: HAuCl$_4$•3H$_2$O (49% Au basis), trisodium citrate (99%) and 1-dodecanethiol (98%) were purchased from Sigma-Aldrich. Single-stranded DNA binding (SSB) protein was purchased from Molecular Cloning Labs, Inc. Milli-Q water was used in all experiments. All glassware was cleaned with acetone, rinsed with deionized water in an ultrasonic bath, and stored at 45°C in a drying oven before use. The quartz slides in the size of 19×20 mm^2 were used as substrates, which were soaked in nitrohydrochloric acid for 12 h. After that, slides were dried with compressed N$_2$ and treated with a plasma cleaner to increase their hydrophilicity immediately before use.

Synthesis of gold nanoparticles: The synthesis process of gold nanoparticles refers to Neus G. Bastus el al.[34] 300 ml of 2.2 mM trisodium citrate was heated under vigorous stirring. 2 ml of 25 mM $HAuCl_4$ solution was added after boiling. The resulting nanoparticles were synthesized in 15 min. The first step solution was called S-1. Then another 2 ml of 25 mM $HAuCl_4$ solution was injected into S-1 until the reaction reached $90^{o}C$. After 30 min, we added the third 2 ml of 25 mM $HAuCl_4$ solution under the temperature of $90^{o}C$. After 30 min, we got S-2 solution. And then, the sample was diluted by extracting 150 ml S-2 solution mixed with 145 ml water and 5 ml 65 mM trisodium citrate. The process was repeated twice by adding 2.7 ml of 25 mM $HAuCl_4$ solution to get S-3 solution. Three different solutions corresponded to gold nanoparticles with three different sizes.

Discontinuous Vertical Evaporation-driven Colloidal Deposition (dVECD): The experimental setup was illustrated in Fig. 1a. A 15 ml beaker containing 10 ml gold nanoparticle colloid solution and a 10 ml syringe were fixed on a shock-absorbing platform at room temperature and atmospheric press. A hydrophilic quartz substrate was vertically immersed into the gold nanoparticle dispersion and kept stationary. Driven by solid-liquid-gas interface force and evaporation, gold nanoparticles were deposited at the interface region with the shape of the liquid level. After a 10 min deposition, the solution level was lowered by a rapid withdrawing of 1 ml solution for achieving a wire-like structure. The repetition of this process causes formation of parallel nanoparticle wires on the substrate. The interval distance between adjacent wires was ~1.5 mm (Fig. 4b).

Characterization of gold nanoparticle wires: Gold nanoparticles were characterized by a transmission electron microscopy (TEM, FEI T20) at 20 keV (Fig. 2d-f). The 10 μl droplet of the 10-time diluted sample was casted onto a piece of ultrathin carbon-coated 200-mesh grid. The surface morphology of GNPWs was observed by a scanning electron microscopy (SEM, FEI nano430).

Gold nanoparticle wires processing: The annealing process was performed in a stove for 4 h. The temperature for 14 nm GNPWs was 120°C, while 150°C and 170°C of 4 h were used for 27 nm GNPWs and 37 nm GNPWs respectively. After that, GNPWs were exposed to a 10 mM 1-dodecanethiol (DDT) in ethanol for 12 h, which neutralizes the surface charge of gold nanoparticles. And then, GNPWs were rinsed by ethanol and water and dried with compressed N$_2$.

Electrical measurement: After deposition of 70 nm gold electrodes by the electron beam evaporation, the resistance measurement of GNPWs was performed by a semiconductor parameter analyzer (KEITHLEY 4200) with a probe station system from -0.2 *V* to 0.2 *V*. We obtained the resistance from the *I-V* curve.

Acknowledgements

Notes and references

[a] State Key Laboratory for Mesoscopic Physics, School of Physics, Peking University, Beijing 100871, P. R. China.

[b] Collaborative Innovation Center of Quantum Matter, Beijing, China. E-mail: zhaoqing@pku.edu.cn

[c] Center for Mitochondrial Biology and Medicine, The Key Laboratory of Biomedical Information Engineering of Ministry of Education, School of Life Science and Technology and Frontier Institute of

Life Science, Frontier Institute of Science and Technology (FIST), Xi'an Jiaotong University, Xi'an 710049, P. R. China. E-mail: diaojj@mail.xjtu.edu.cn

d University of North Carolina at Chapel Hill, Chapel Hill, NC 27599, USA

e SK hynix memory solutions, 3103 North First Street, San Jose, CA 95134, USA

1. Y. Huang, X. Duan, Q. Wei and C. M. Lieber, *Science*, 2001, **291**, 630-3.

2. J. J. Diao and H. Chen, *J. Chem. Phys.*, 2006, **124**, 116103.

3. V. Santhanam and R. P. Andres, *Nano Lett.*, 2004, **4**, 41-44.

4. J. J. Diao and G. D. Chen, *J. Phys. D: Appl. Phys.*, 2001, **34**, L79-L82.

5. K. H. Bhatt and O. D. Velev, *Langmuir*, 2004, **20**, 467-476.

6. S. A. Maier, P. G. Kik, H. A. Atwater, S. Meltzer, E. Harel, B. E. Koel and A. A. Requicha, *Nat. Mater.*, 2003, **2**, 229-32.

7. Q. H. Wei, K. H. Su, S. Durant and X. Zhang, *Nano Lett.*, 2004, **4**, 1067-1071.

8. Y. Yin, Y. Lu and Y. Xia, *J. Am. Chem. Soc.*, 2001, **123**, 771-772.

9. L. M. Demers, D. S. Ginger, S. J. Park, Z. Li, S. W. Chung and C. A. Mirkin, *Science*, 2002, **296**, 1836-8.

10. C. R.Barry, N. Z. Lwin, W. Zheng and H. O. Jacobs, *Appl. Phys. Lett.*, 2003, **83**, 5527-5529.

11. Y. Cui, M. T. Björk, J. A. Liddle, C. Sönnichsen, B. Boussert and A. P. Alivisatos, *Nano Lett.*, 2004, **4**, 1093-1098.

12. O. Velev and E. Kaler, *Langmuir*, 1999, **15**, 3693-3698.

13. C. A. Mirkin, R. L. Letsinger, R. C. Mucic and J. J. Storhoff, *Nature*, 1996, **382**, 607-609.

14. W. Shenton, S. A. Davis and S. Mann, *Adv. Mater.*, 1999, **11**, 449-452.

15. K. D. Hermanson, S. O. Lumsdon, J. P. Williams, E. W. Kaler and O. D. Velev, *Science*, 2001, **294**, 1082-6.

Nanoscale Accepted Manuscript

16. D. J. Norris and Y. A. Vlasov, *Adv. Mater.*, 2001, **13**, 371-376.

17. Y. Y. Pinto, J. D. Le, N. C. Seeman, K. Musier-Forsyth, T. A. Taton and R. A. Kiehl, *Nano Lett.*, 2005, **5**, 2399-2402.

18. S. Kwon, X. Yan, A. M. Contreras, J. A. Liddle, G. A. Somorjai and J. Bokor, *Nano Lett.*, 2005, **5**, 2557-2562.

19. S. Vyawahare, K. M. Craig and A. Scherer, *Nano Lett.*, 2006, **6**, 271-276.

20. J. Diao, J. Sun, J. Hutchison and M. Reeves, *Appl. Phys. Lett.*, 2005, **87**, 103113-103113-3.

21. J. Huang, F. Kim, A. R. Tao, S. Connor and P. Yang, *Nat. Mater.*, 2005, **4**, 896-900.

22. J. Huang, A. R. Tao, S. Connor, R. He and P. Yang, *Nano Lett.*, 2006, **6**, 524-529.

23. P. T. Anastas, J. C. Warner, *Green Chemistry: Theory and Practice*. Oxford University Press: New York, 1998.

24. J. A. Dahl and P. Collas, *Front Biosci.*, 2007, **12**, 4925-4931.

25. K. Müller, G. Wei, B. Raguse and J. Myers, *Phys. Rev. B*, 2003, **68**, 155407.

26. C. M. Guedon, J. Zonneveld, H. Valkenier, J. C. Hummelen and S. J. van der Molen, *Nanotechnology*, 2011, **22**, 125205.

27. J. J. Diao and Q. Cao, *AIP Advances*, 2011, **1**, 012115.

28. C. Farcau, N. M. Sangeetha, H. Moreira, B. Viallet, J. Grisolia, D. Ciuculescu-Pradines and L. Ressier, *ACS Nano*, 2011, **5**, 7137-7143.

29. C. Farcau, H. Moreira, B. Viallet, J. Grisolia, D. Ciuculescu-Pradines and C. Amiens, L. Ressier, *J. Chem. Phys. C*, 2011, **115**, 14494-14499.

30. S. Watanabe, Y. Mino, Y. Ichikawa and M. T. Miyahara, *Langmiur*, 2012, **28**, 12982-12988.

31. S. Watanabe, K. Inukai, S. Mizuta and M. T. Miyahara, *Langmuir*, 2009, **25**, 7287-7295.

32. G. K. Chan and T. Van Voorhis, *J Chem. Phys.*, 2005, **122**, 204101.

33. J. J. Diao and M. G. Xia, *Colloid Surf. A: Physicochem. Eng. Asp.*, 2009, **338**, 167-170.

34. N. G. Bastus, J. Comenge and V. Puntes, *Langmuir*, 2011, **27**, 11098-11105.

35. J. Yang, T. Ichii, K. Murase and H. Sugimura, *Langmuir*, 2012, **28**, 7579-84.

36. M. Garcia, J. de la Venta, P. Crespo, J. Llopis, S. Penadés, A. Fernández and A. Hernando, *Phys. Rev. B*, 2005, **72**, 241403.

37. Y. Cui, Q. Wei, H. Park and C. M. Lieber, *Science*, 2001, **293**, 1289-1292.

38. F. Patolsky, G. Zheng, O. Hayden, M. Lakadamyali, X. Zhuang and C. M. Lieber, *Proc. Natl. Acad. Sci. USA*, 2004, **101**, 14017-22.

39. Y. Chen, G. Luo, J. Diao, O. Chornoguz, M. Reeves and A. Vertes, *J. Phys. Conference Series*, 2007, **59**, 548-544.

40. Z. Sun, W. Qiang, H. Li, N. Hao, D. Xu and H.-Y. Chen, *Analyst*, 2011, **136**, 540-544.

41. K. H. Müller, J. Herrmann, B. Raguse, G. Baxter and T. Reda, *Phys. Rev. B*, 2002, **66**, 075417.

42. H.-O. Müller, K. Katayama and H. Mizuta, *J. Appl. Phys.*, 1998, **84**, 5603-5609.

43. D. Porath, A. Bezryadin, S. De Vries and C. Dekker, *Nature*, 2000, **403**, 635-638.

44. Y. Okahata, T. Kobayashi, K. Tanaka and M. Shimomura, *J. Am. Chem. Soc.*, 1998, **120**, 6165-6166.

45. T. M. Lohman and M. E. Ferrari, *Annu. Rev. Biochem.*, 1994, **63**, 527-570.

46. C. Wang, J. Huang, J. Wang, C. Gu, J. Wang, B. Zhang and J. Liu, *Colloids Surf. B: Biointerfaces*, 2009, **69**, 99-104.

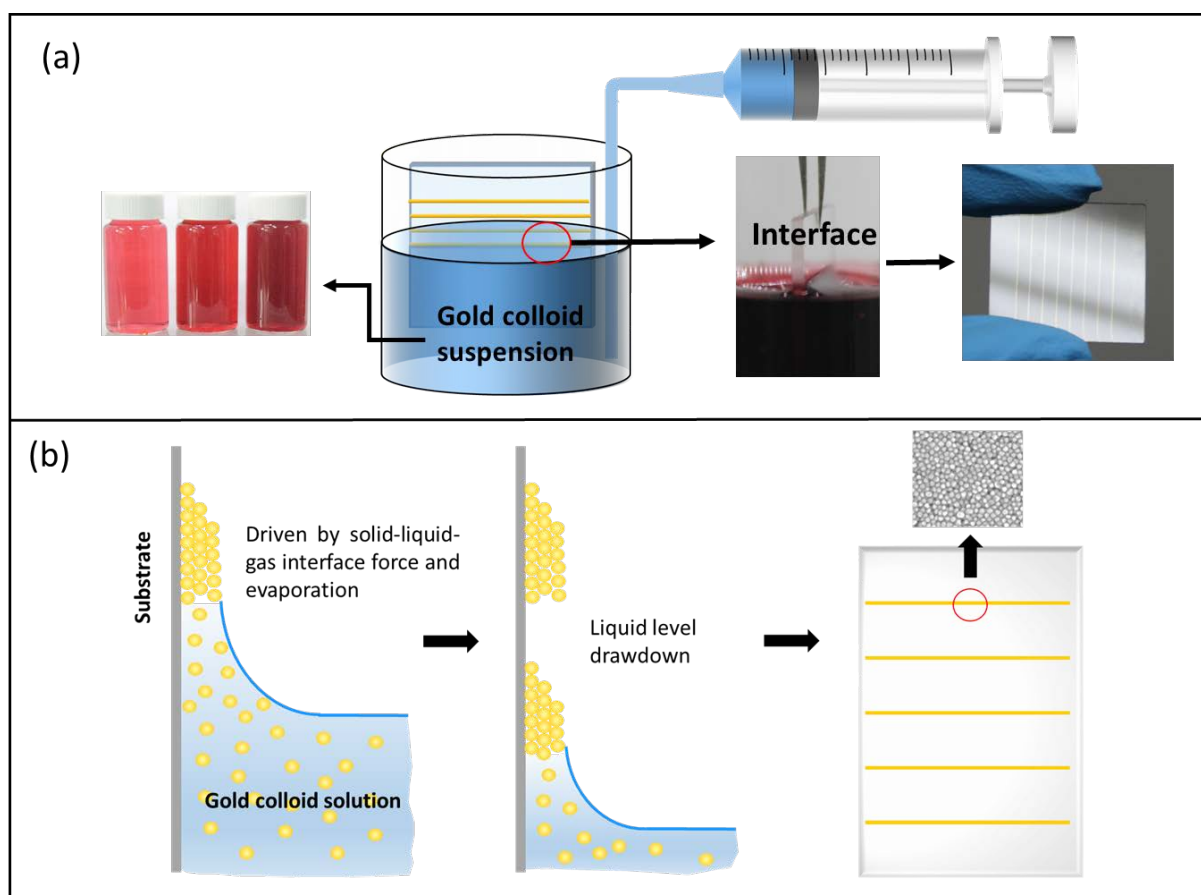47. S-J. Park, T. A. Taton and C. A. Mirkin, *Science*, 2002, **295**, 1503-1506.

Fig.1 (a) Scheme of parallel gold nanoparticle wires formation by dVECD with withdrawing certain amount of liquid solution through a syringe. Gold nanoparticles in different sizes (the left photograph showing three colors of gold colloid solution) were used in our experiment. Two photographs in the right show the solution-air-substrate interface where the gold nanoparticle wire was deposited, and a typical substrate after eight wires had been fabricated. (b) Scheme of the principle of dVECD for the formation of gold nanoparticle wires (GNPWs) driven by solid-liquid-gas interface force and evaporation. A "wire" was finished by rapid liquid level drawdown. Parallel nanoparticle wires were formed with the repetition of this process.
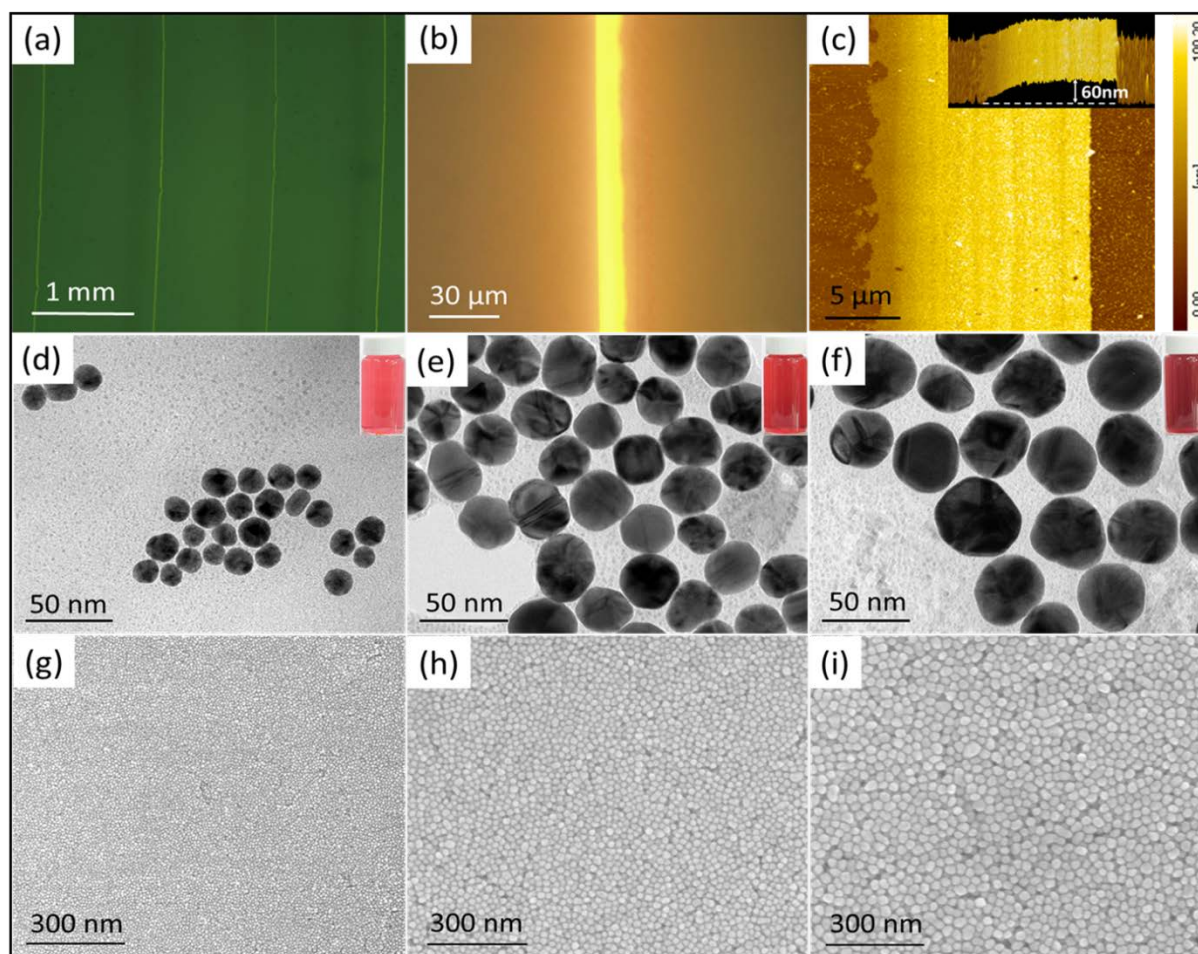
Fig. 2 (a) and (b) are optical microscope images of gold nanoparticle wires, while (c) is an atomic force microscopy (AFM) image. The width of the wire is ~12 μm and the height is ~60 nm. The nanoparticle size in (a), (b), and (c) is 26.57 ± 2.69 nm as typical examples. Gold nanoparticles with different sizes, shown by transmission electron microscopy (TEM) images for diameters of (d) 14.01 ± 1.68, (e) 26.57 ± 2.69, and (f) 36.64 ±2.43 nm, were used for deposition on quartz surface with a 10-min deposition. The insets are the corresponding gold colloid solution. The corresponding surface morphology of gold nanoparticle wires were illustrated by scanning electron microscopy (SEM) in (g), (h), and (i), respectively.
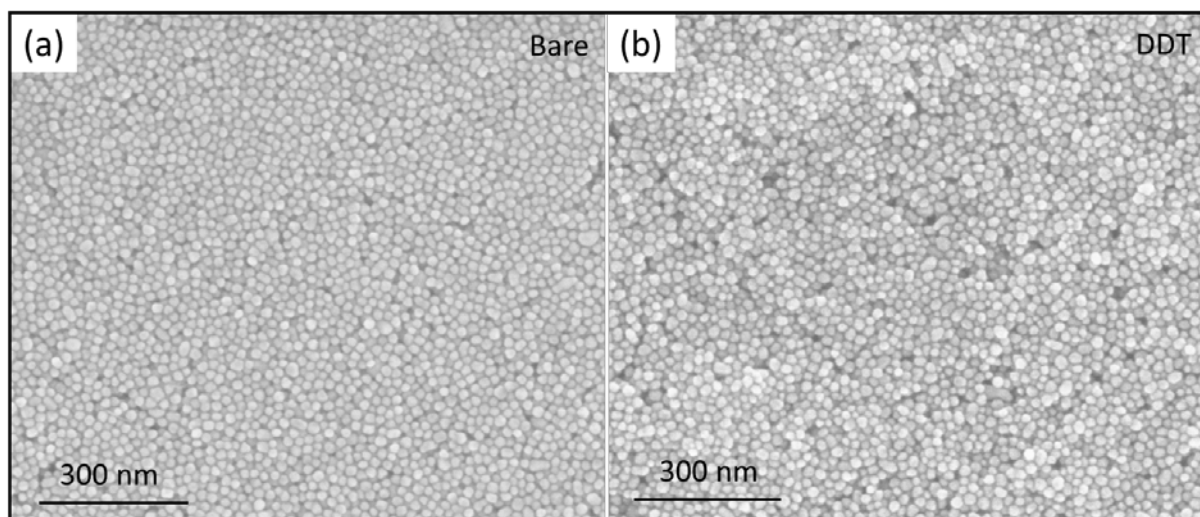
Fig. 3 SEM images of 27 nm GNPWs before (a) and after DDT treatment (b), showing that DDT treatment results in a rougher surface.
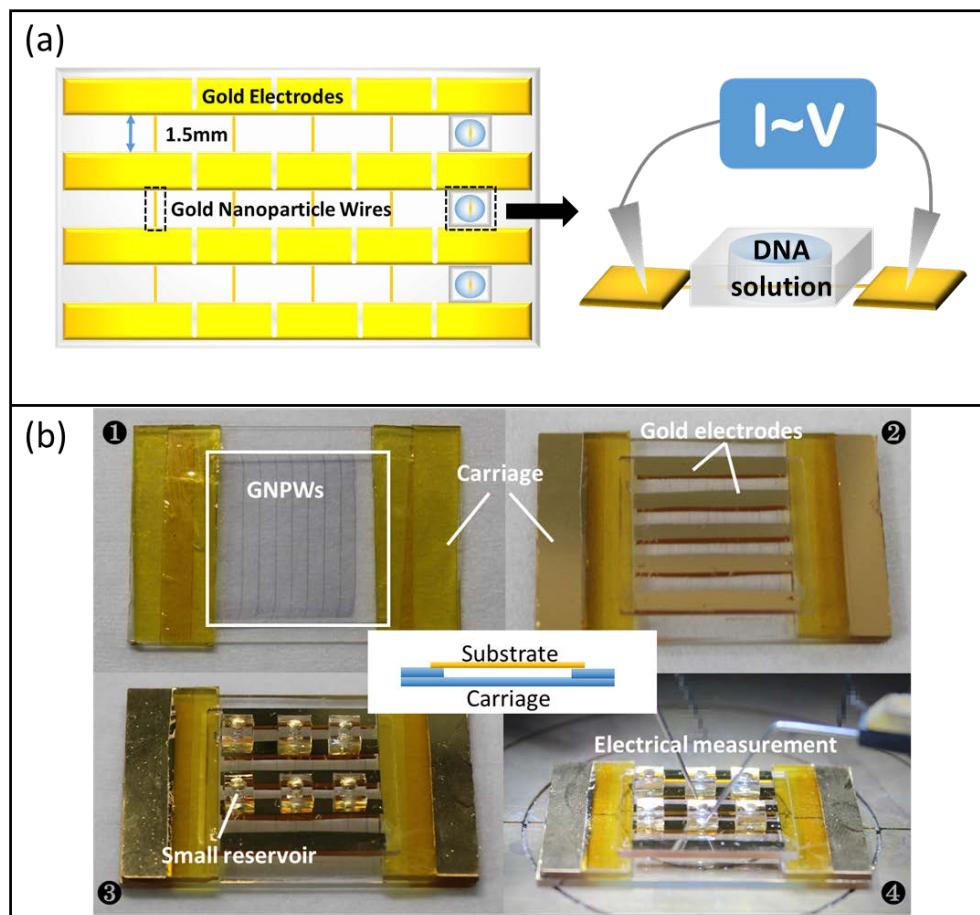
Fig. 4 (a) Schematic of the DNA sensing system based on gold nanoparticle wires. 5*3 sensing devices were fabricated by gold electrode deposition and disconnection. Among them, three devices with reservoir attachment for DNA solution loading were shown, indicated with the dashed black square. A zoom-in scheme (right) shows the electrical resistance measurement through the two gold electrodes connected by the wire and solution. (b) Photographs showing the steps of formation of gold nanoparticle wires sensing device for detection of molecules. 1. Preparation of sensing chambers by supporting the substrate with carriage. 2. Deposition of 70 nm gold electrode by electron beam evaporation. 3. Attachment of small reservoirs to GNPWs to contain DNA samples. 4. Electrical measurement through two probes. The inset is the design of a carriage for using GNPWs in both sides of the substrate.
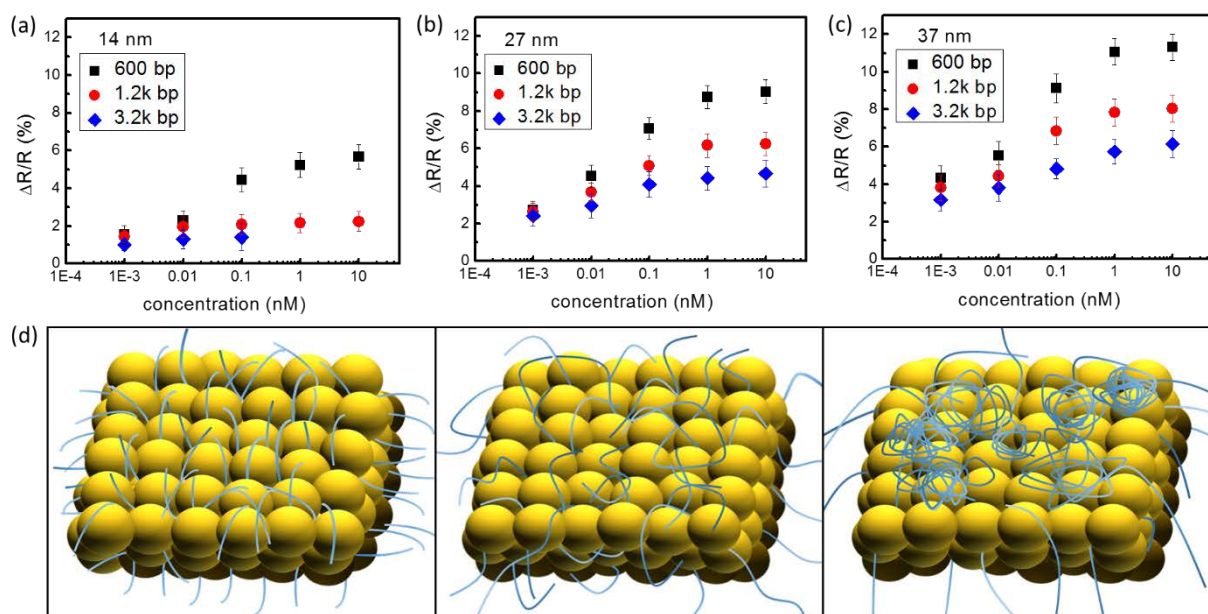
Fig. 5 Nanoparticle wires made with different sizes of gold nanoparticles were utilized for electronic detection of DNAs. Resistance changes of (a) 14, (b) 27, and (c) 37 nm GNPWs upon exposing to different length of double-stranded DNAs (dsDNAs, 600 bp, 1.2 kbp, and 3.2 kbp) at different DNA concentrations. The increased nanoparticles gave gradually larger ΔR/R variation values. (d) Schematic illustration shows a better insertion for shorter DNAs in between nearby particle gaps.
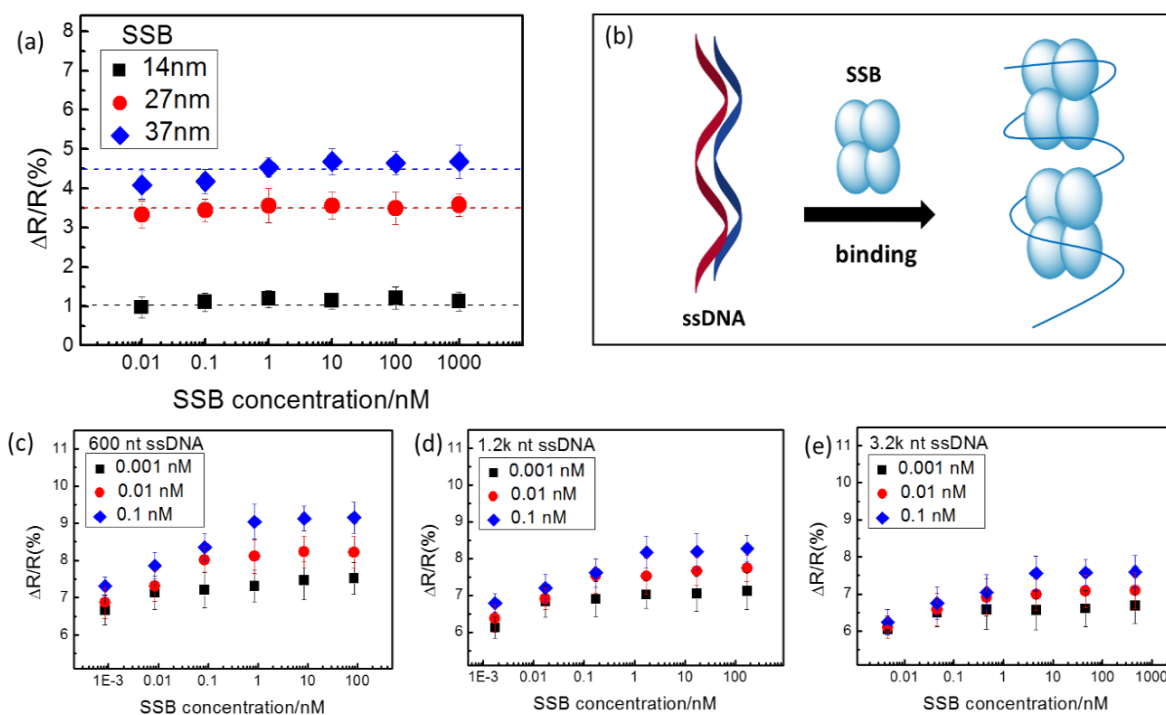
Fig. 6 (a) The resistance changes of 14, 27, and 37 nm gold nanoparticle wires after adding single-stranded DNA binding protein (SSB) at different SSB concentrations. No significant change was detected as a function of concentration. (b) The interaction sketch for single-strand DNAs and SSB. (c), (d) and (e): ΔR/R values for ssDNAs (600 nt, 1200 nt, 3200 nt) upon binding with SSB as a function of SSB concentrations. 37 nm GNPWs were used under three ssDNA concentrations (0.001 nM, 0.01 nM, 0.1 nM).